IJSRM
INTERNATIONAL JOURNAL OF SCIENCE AND RESEARCH METHODOLOGY
An Official Publication of Human Journals

Human Journals
Research Article
June 2018 Vol.:9, Issue:4

Numerical Study of Natural Convection in a Cylindrical Vertical Channel with Mass Deposition Simulating a Thermosiphon

IJSRM
INTERNATIONAL JOURNAL OF SCIENCE AND RESEARCH METHODOLOGY
An Official Publication of Human Journals

Ousman Rilengar Godfroyd*[1,2], Zeinebou Mint Sidi[1], Cheikh Mbow[1], Aboubaker Chedikh Beye[3]

[1] *Fluid Mechanics and Applications Laboratory, Cheikh Anta Diop University, Dakar, Senegal*

[2] *Fluid Mechanics and Applications Laboratory, Mongo Polytechnic University, Chad*

[3] *Physics Solid and Materials Sciences Laboratory, Cheikh Anta Diop University, Dakar, Senegal.*

Submission: 22 May 2018
Accepted: 29 May 2018
Published: 30 June 2018

Keywords: Digital Analysis, Natural Convection, Fortran, Vertical Cylinder, Thermosiphon

ABSTRACT

In this study, we have developed a theoretical model representing the vertical channel from a vertical cylinder open at both ends and having a heat source heated to imposed heat flux. This source is placed at the entrance of the cylinder and the vertical walls of the cylinder maintained adiabatic. The equations governing the hydrodynamic flow, the heat transfer and the species are described by the Navier Stockes equations, the energy equation and the species in the verticity-current function formulation. These equations are discretized by the finite volume method and the coefficients of the algebraic equation are approximated by the power law scheme. Numerical simulations are performed in the case of binary fluid for a Grashof number equal to 10^5; a form factor of 0.5, the source radius is 0.125. The results show that close to the heating plate, the temperature gradient is strongly accentuated, resulting in a strong aspiration of the ambient air; there is then an area where the stratification due to the buoyancy effect develops and a zone where the temperature gradient decreases until the total establishment of the flow. Mass deposition is organized in proportion to the longitudinal variation of the temperature gradient. The transverse velocity profiles are almost not observed because the flow is strongly influenced longitudinally and also, the heating plate constitutes an obstacle to the circulation; this is explained by a return flow.

1-INTRODUCTION

Nowadays, natural convection heat transfer in open enclosures can be applied in various industrial processes such as the cooling of electronic equipment, the cooling of printed circuits, the discharge of fumes at the exit of industrial chimneys, etc. The phenomenon of thermosiphon has been the subject of several studies around the world. In exploring the structure of the flow inside a heated cylinder, [1] has shown that during the vertical evolution, three different zones have been identified: (i) a zone, serving to feed the plume in fresh air with a high temperature gradient close to the heating plate, (ii) a zone of development of the flow due to the buoyancy effect and (iii) a zone of establishment of the flow. [3] and [4] have shown that at the entrance of the system, the vertical speed is important in the central part and that as the height increases, the speed becomes more and more intense near of the wall and increasingly weak in the central part of the cylinder. In addition, other works such as those of [5-6] have highlighted the importance of the volume flow of air sucked by the thermosiphon. These authors have subsequently proposed empirical laws connecting the flow rate of the circulating fluid in the cylinder and Rayleigh number for different flow regimes. The change in parental boundary conditions at the source of the plume due to the effect of the thermosiphon could be at the origin of a possible change in the flow structure. [7-14] have had this simulated turbulent flow in the laboratory, in the structure of the plume generated by the source. The results obtained in this case made it possible to distinguish, during the vertical evolution of the plume, two different zones: the first which characterizes the development of turbulence and the second which is the seat of a fully established turbulent flow. Numerous numerical and experimental studies have been carried out separately for free and unlimited thermal plume flows [16-17], or thermosiphon flows [17-19]. Our study follows the continuity of [1] which is inspired by the experimental study of [19] which experimentally studied the effects of thermosiphon on the dispersion of pollutants. In this work, we studied the flow of fluid inside an open cylinder at both ends and subjected to an imposed heat flow heating plate. The cylinder is of height H, factor A = 0.5, and the radius of the source is R * = 0.125. Our calculations were made from a FORTRAN code developed for this purpose. Originpro.8 software was then used for the exploitation of the numerical results. The objective of this study is to evaluate the various flow control parameters in the vertical cylinder open at both ends with mass deposition, for industrial applications. The results obtained are overall consistent and revealing.

2- MATERIALS AND METHODS

2-1-Problematic

To model the transfer mechanisms involved in the system, we considered the cylinder shown schematically in **Figure 1** below. Our goal is to predict what happens in the chimney when setting boundary conditions at the inlet and outlet of the cylinder and the conditions on the vertical walls.

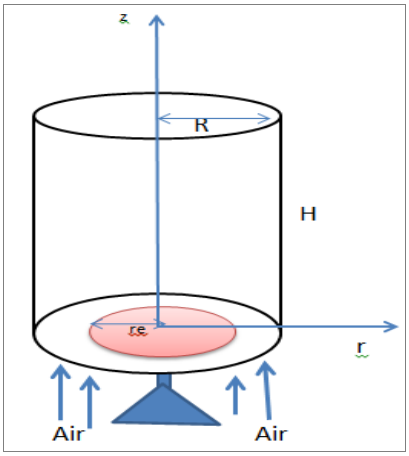

Fig.1-Geometric configuration of the problem

2-2-Mathematical model

In order to facilitate the equation and the numerical treatment, we have formulated the following simplifying hypotheses: (i) the binary fluid is an incompressible Newtonian fluid, (ii) the generated flow is laminar; (iii) the flow satisfies the Boussinesq approximation, this approximation assumes that the thermophysical quantities of the binary mixture are constant with the exception of the density of the mixture in the term of natural convection generating force where the mass volume is given for a binary fluid by:

$$\rho = \rho_L \left[1 - \beta_T (T - T_L) - \beta_C (C - C_L)\right] \qquad (1)$$

$$\beta_T = -\frac{1}{\rho_L}\left(\frac{\partial \rho}{\partial T}\right)_C \text{ and } \quad \beta_C = -\frac{1}{\rho_L}\left(\frac{\partial \rho}{\partial C}\right)_T$$

β_T and β_T are respectively the coefficients of thermal and mass expansion of the binary fluid, the temperature and the mass fraction of the heaviest constituent. Values of these quantities in the state of reference). The general vector equations of conservation of the binary fluids are written:

$$\frac{\partial \rho}{\partial t} + \rho \vec{\nabla}.\vec{V} = 0 \qquad (2)$$

$$\frac{\partial}{\partial t}(\rho \vec{V}) + \rho \nabla.\vec{V} = \rho \vec{g} - \nabla P + \mu \nabla^2 \vec{V} \qquad (3)$$

$$\frac{dT}{dt} - \frac{k}{\rho C_P} \nabla^2 T = 0 \qquad (4)$$

$$\frac{dC}{dt} - D\nabla^2 C = S(C,T) \qquad (5)$$

The evolution of the fields (speed, temperature and solute concentration) is constrained by the conservation laws (of momentum, mass, energy and chemical species). For an inert incompressible binary liquid, these equations are obtained using the dimensionless variables defined as follows:

$$r' = \frac{r}{H}, z' = \frac{z}{H}, \quad t' = \frac{Vr}{R}t, \quad \theta = \frac{T - T_0}{\Delta T_r} \quad u' = \frac{U}{V_r}, v' = \frac{V}{V_r}, C = \frac{C - C_0}{\Delta C_r}$$

The conservation equations of mass, momentum, concentration and adimensionnated energy in bidimensional cylindrical coordinate are then written:

$$\frac{1}{r}\frac{\partial (rU)}{\partial r} + \frac{\partial V}{\partial z} = 0 \qquad (6)$$

$$\frac{\partial U}{\partial t} + \left(U\frac{\partial U}{\partial r} + V\frac{\partial U}{\partial z} \right) = -\frac{\partial P}{\partial r} + \frac{1}{\mathrm{Re}}\left[\frac{1}{r}\frac{\partial}{\partial r}\left(r\frac{\partial U}{\partial r} \right) + \frac{\partial^2 U}{\partial z^2} \right] \qquad (7)$$

$$\frac{\partial V}{\partial t}+\left(U\frac{\partial V}{\partial r}+V\frac{\partial V}{\partial z}\right)=-\frac{\partial P}{\partial z}+\frac{1}{\mathrm{Re}}\left[\frac{1}{r}\frac{\partial}{\partial r}\left(r\frac{\partial V}{\partial r}\right)+\frac{\partial^2 V}{\partial z^2}-\frac{V}{r^2}\right] -\frac{Gra_T.\theta}{\mathrm{Re}^2}-\frac{Gra_m.C}{\mathrm{Re}^2} \quad (8)$$

$$\frac{\partial \theta}{\partial t}+\left(U\frac{\partial \theta}{\partial r}+V\frac{\partial \theta}{\partial z}\right)=\frac{1}{pe_t}\left[\frac{1}{r}\frac{\partial}{\partial r}\left(r\frac{\partial \theta}{\partial r}\right)+\frac{\partial^2 \theta}{\partial z^2}\right] \quad (9)$$

$$\frac{\partial C}{\partial t}+\left(U\frac{\partial C}{\partial r}+V\frac{\partial C}{\partial z}\right)=\frac{1}{Pe_m}\left[\frac{1}{r}\frac{\partial}{\partial r}\left(r\frac{\partial C}{\partial r}\right)+\frac{\partial^2 C}{\partial z^2}\right] +\Sigma(\theta,C) \quad (10)$$

The verticity-current function formulation offers the advantage of eliminating the pressure and automatically checking the continuity equation. A current function is introduced by asking:

$$U=-\frac{1}{r}\frac{\partial \psi}{\partial z};\quad V=\frac{1}{r}\frac{\partial \psi}{\partial r};\quad \omega=\frac{\partial U}{\partial z}-\frac{\partial V}{\partial r} \quad (11)$$

$$\frac{1}{r}\frac{\partial^2 \psi}{\partial z^2}+\frac{\partial}{\partial r}\left(\frac{1}{r}\frac{\partial \psi}{\partial r}\right)=-\omega \quad (12)$$

$$\frac{\partial \omega}{\partial t}-\frac{\partial \omega}{\partial r}\left(\frac{1}{r}\frac{\partial \psi}{\partial z}\right)+\frac{\partial \omega}{\partial z}\left(\frac{1}{r}\frac{\partial \psi}{\partial r}\right)=\frac{1}{\mathrm{Re}}\left[\frac{1}{r}\frac{\partial}{\partial r}\left(r\frac{\partial \omega}{\partial r}\right)+\frac{\partial^2 \omega}{\partial z^2}-\frac{\omega}{r^2}\right] + \frac{Grat}{\mathrm{Re}^2}.\frac{\partial \theta}{\partial r} \quad (13)$$

$$\frac{\partial \theta}{\partial t}-\frac{1}{r}\frac{\partial \psi}{\partial z}\frac{\partial \theta}{\partial r}+\frac{1}{r}\frac{\partial \psi}{\partial r}\frac{\partial \theta}{\partial z}=\frac{1}{pe_t}\left[\frac{1}{r}\frac{\partial}{\partial r}\left(r\frac{\partial \theta}{\partial r}\right)+\frac{\partial^2 \theta}{\partial z^2}\right] \quad (14)$$

$$\frac{\partial C}{\partial t}-\frac{1}{r}\frac{\partial \psi}{\partial z}\frac{\partial C}{\partial r}+\frac{1}{r}\frac{\partial \psi}{\partial r}\frac{\partial C}{\partial z}=\frac{1}{pe_m}\left[\frac{1}{r}\frac{\partial}{\partial r}\left(r\frac{\partial C}{\partial r}\right)+\frac{\partial^2 C}{\partial z^2}\right] +\Sigma(\theta,C) \quad (15)$$

2-3-Border and boundary conditions

✓ Initial conditions

A t=0, $\theta(r,z,0)=0, C(r,z,0)=0, \vec{V}(r,z,0)=\vec{0}$

$$\psi(r,z,0)=0, \omega(r,z,0)=0 \qquad (16)$$

✓ Condition at the entrance:

$$\begin{cases} \vec{V}(r,0,t)=\vec{0}, \\ \dfrac{\partial\theta}{\partial z}=-1 \end{cases} \qquad (17)$$

✓ Thermal and mass conditions

$$\theta(r,0,t)=0, \quad C(r,0,t)=0 \qquad (18)$$

Condition on the walls of the pipe:

$$\frac{\partial\theta(R,z,t)}{\partial z}=0, \quad \frac{\partial C(r,z,t)}{\partial z}=0 \qquad (19)$$

✓ Conditions on speed, current function and output verticity:

$(z=H, \quad O' \prec z \leq R)$

$$\begin{cases} si\ \vec{V}.\vec{e_z} \leq 0, \quad , \quad \theta=0 \quad , \quad C=C_{ext} \\ si \quad \vec{V}.\vec{e_z} \geq 0, \dfrac{\partial U}{\partial z}=\dfrac{\partial V}{\partial z}=\dfrac{\partial\theta}{\partial z}=\dfrac{\partial C}{\partial z} \end{cases} \qquad (20)$$

✓ Hydrodynamic conditions

$$\frac{\partial U}{\partial r}=\frac{\partial V}{\partial r}=\frac{\partial\psi}{\partial r}=\frac{\partial\omega}{\partial r}=0 \qquad (21)$$

3-Validation

In this work, the results of the article [1] were used. For this, we considered the same conditions (the Grashof number is taken at $Gra_T = 10^5$, the shape ratios and the radius of the hot source are respectively A = 0.5 and R * = 0.125).

4-RESULTS AND DISCUSSIONS

4-1-Variable Z thermal and dynamic fields

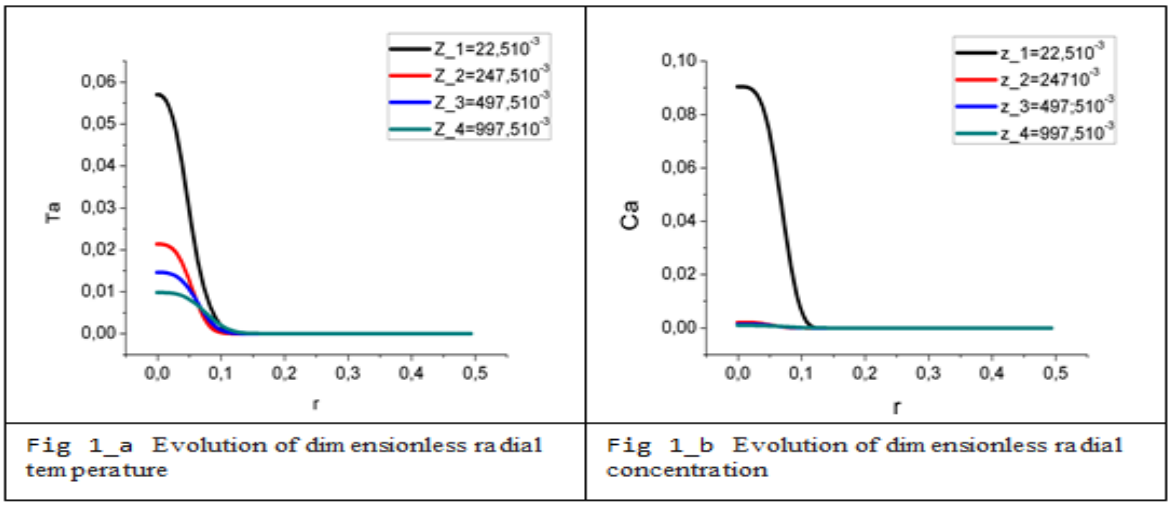

Fig 1_a Evolution of dimensionless radial temperature

Fig 1_b Evolution of dimensionless radial concentration

Fig.1-Evolution of temperature and adimensional radial concentration

Fig.1a presents the radial distribution of the dimensionless temperature of the flow at different levels Z. Indeed, in the zone close to the hot source ($Z \leq 0.2475$), the temperature profile presents a maximum situated on the axis of symmetry. The presence of a strong temperature gradient is noted. In the meantime ($0.2475 < Z < 0.9975$), the temperature gradient becomes less important. This shows temperature profiles that are decreasing in relation to the vertical. In the last zone ($Z = 0.9975$), the temperature profiles fall, become self-similar and almost identical to show the total establishment of the temperature flow. Fig.1b shows that the mass deposition is proportional to the variation of the temperature until the total establishment.

The evolution of the adimensional longitudinal radial velocity of the flow at different levels Z is given in (Fig. 2c). Longitudinal velocity profiles present three different aspects of the overall flow structure. In fact, for the zones located near the hot source ($Z < 0.2475$) the

velocity profiles evolve slowly with a maximum located largely in the center of the cylinder at (R * = 0.5). This structure is due to the fact that the fluid layers arriving from outside, at room temperature and denser, are located above the warmer and lighter layers, adjacent to the hot surface of the source. This is a potentially unstable stratification, which gives rise to a convective motion.

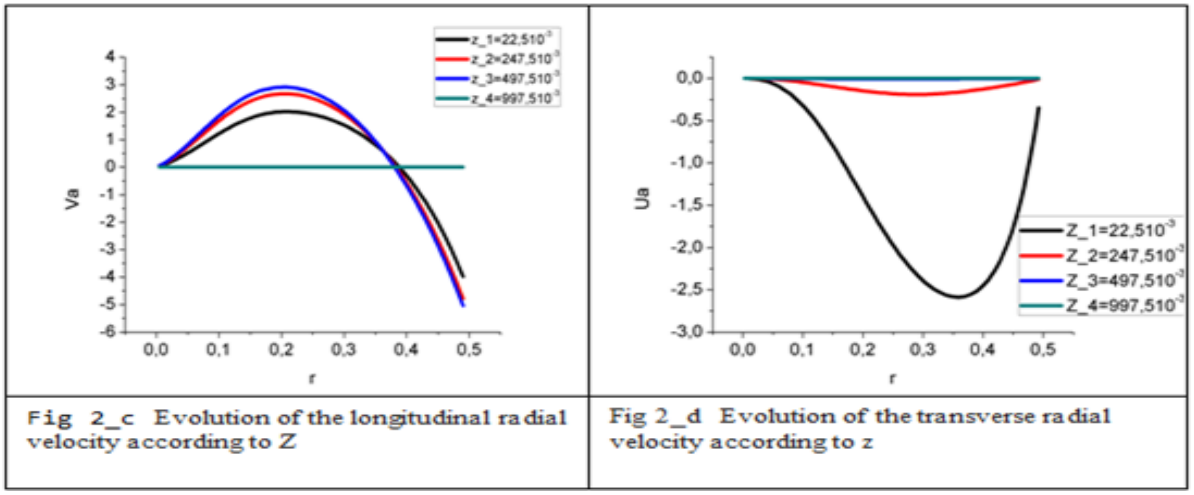

Fig 2_c Evolution of the longitudinal radial velocity according to Z

Fig 2_d Evolution of the transverse radial velocity according to z

Fig.2-Evolution of the longitudinal and transverse radial velocity e according to z

In the intermediate zone, (0.2475 ≤ Z <0.9975), we observe the appearance of a new flow structure where the velocity profiles have a minimum approaching the end of the source radius, of the source (re = 0.125). This is a competition between Archimedes' push forces and viscous forces. In the area moving towards the exit of the cylinder (0.2475 <Z ≤ 0.9975), the equilibrium between the buoyancy forces of Archimedes and viscous is reached. A maximum is reached, then the temperature gradients become smaller and smaller, which slows down the flow rate until the flow is fully established. Fig. 2 (d) confirms that the fluid does not leave our theoretical model; this is explained by the total establishment of the transverse radial velocity at the outlet of the cylinder at z = 0.9975. A negative return flow confirms that the movement is preferentially oriented along the z-axis. So the effects of the transversal speed are not taken into account.

4-2- Isothermal and mass value networks t = 10^{-5}

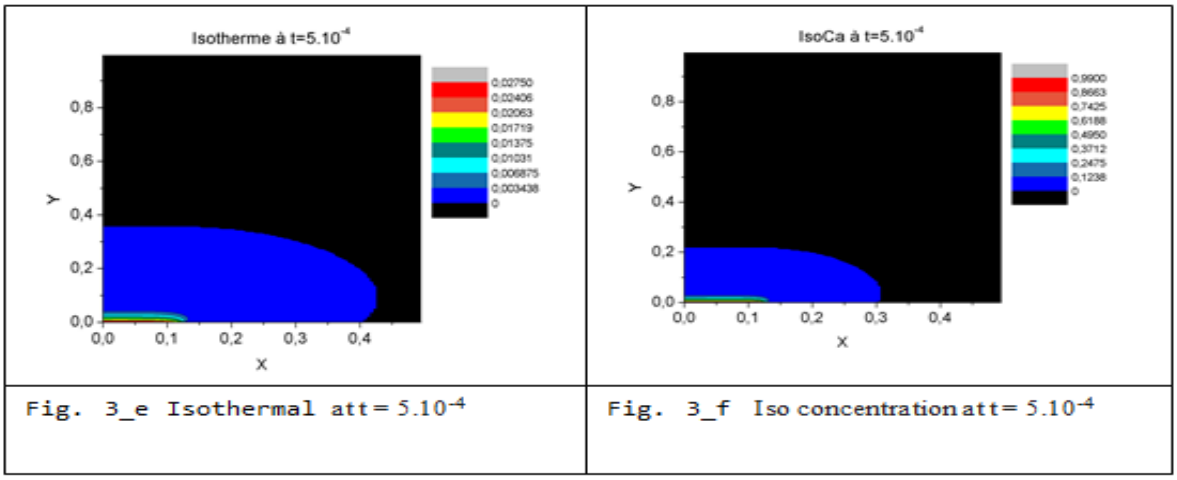

Fig. 3_e Isothermal att= 5.10^{-4} | Fig. 3_f Iso concentration att= 5.10^{-4}

Fig. 3-Thermal and mass iso values

FIG. 3 obtained the result obtained with respect to the mass deposit inside the studied system. On the immediate remark even t = 5 $.10^{-4}$, (fig.3e) shows a strong temperature gradient which changes the fluid sucked from the outside into a strongly accentuated thermal plume. This phenomenon to be aroused in (fig.3d), an onset of mass deposition by reducing the quantity of the inside of the cylinder.

5- CONCLUSION

In this paper, we studied the flow of fluid with mass deposition inside a cylinder open at both ends and subjected to an imposed heat flow heating plate. For calculation purposes, a program under FORTRAN has been implemented. Origin Pro.8 software was then used for their graphical results. Our objective through this study is to evaluate the natural convection flows with mass deposition inside the studied device. Overall, the results obtained are consistent and revealing. The radial distribution of the temperature made it possible to identify a zone with strong development of the plume generating mass deposition. The radial evolution of the longitudinal velocity revealed three different aspects of the global flow structure: a highly unstable stratification giving rise to a convective motion; the appearance of a new flow structure where the velocity profiles have a maximum of the equilibrium between the force of Archimedes and the viscous force, followed by a decrease of the flow velocity up to the total establishment. The isovalues of the thermal and mass fields confirm

the result obtained with respect to the mass deposit inside the studied system. It should also be noted that the model used in this study is two-dimensional for laminar flow. As the natural flows are mostly turbulent, it would be interesting to confirm these results using a three-dimensional numerical model, in the context of turbulence that can understand the physical phenomenon related to flow and mass deposition.

REFERENCES

[1] Ousman Rilengar G. et al. (2018) Numerical modeling of a natural convection flow in a thermosiphon: Thermal plume, Int. J. Adv. Res. 6 (3), 103-109. http://dx.doi.org/10.21474/IJAR01/6655
[2] Dring R.P., Gebhart B. (1966) Transient natural convection from thin vertical cylinder, J. Heat Trans.-T. ASME 246-248.
[3] Z. Yahya, Ch. Mbow, (2015) Study of the effect of thermosiphon on the vertical dispersion of pollutants, 22nd French Congress of Mechanics Lyon, http://hdl.handle.net/2042/57163
[4] Dalbert A. M.et al. (1981) Laminar natural convection in a vertically heated constant flow channel, lnt. J. Heat Mass Tran. 24 1463-1473.
[5] Ben Maad R., (1995) Study of a natural convection flow in a heated vertical channel, thesis, University of Tunis.
[6] Agator J.·M., Doan K.S. (1982) Turbulent structure of axi-symmetric thermal plume, Mech. Res. Commun. 9 159-1 64.
[7] Agator J.·M., (1983) Contribution to the study of the turbulent structure of a thermal plume with axial symmetry. Interaction of the plume with its limited environment, thesis, University of Poitiers,
[8] Agator J.-M. et al. (1998) Characteristics of thermal turbulence in an axially symmetric plume, J. Mée. Theor. Appl. 3 577-599.
[9] Brahimi M., Doan K.S., (1 986) Experimental and numerical predictions of the mean flow of a turbulent pure plume, Arch. Mech. Warszawa 38 51 9-528.
[10] Brahimi M., (1987) Turbulent structure of thermal plumes-interaction, thesis, University of Poitiers.
[11] Brahimi M. et al. (1998) Medium and fluctuating fields of isolated or interacting thermal plumes, Rev. Brig. Therm. 315-316 236-243.
[12] Brahimi M. et al. (1989) Turbulence structure of the interaction flow of two thermal plumes, int. J. Heat Mass Tran 32 1551-1559.
[13] Dehmani L. et al. (l 996) Influence of strong density stratification on the entrainment of a turbulent axisymmetric plume, Exp. Fluids 21
[14] B. Guillou (1984) Numerical and experimental study of the turbulent structure of a pure plume with axial symmetry, Thesis PhD, University of Poitiers.
[15] J. M. Agator, Doan-Kim-Son, (1983) Spectral analysis of the thermal field of a turbulent plume with axial symmetry, C.R. Acad. Sc. Paris.
[16] C. Kettleborough, (1972) Transient laminar free convection between heated vertical plates including entrance effects, International Journal of Heat and Mass Transfer 15883–896
[17] R. Wirtz, R. Stutzman (1982) Experiments on free convection between vertical plates with symmetric heating, Journal of Heat Transfer 104.
[18] S. Ramanathan, R. Kumar, (1991) Correlations for natural convection between heated vertical plates, Journal of Heat Transfer (Transcations of the ASME (American Society of Mechanical Engineers), SeriesC) United States 113
[19] A. O. M. Mahmoud, et al. (2006) Improvement of the Vertical Dispersion of Pollutants Resulting From Chimneys by Thermosiphon Effect. American Journal of Environmental Sciences 2 66-73.

Nomenclature

Notation	
g	Gravity instensity, $m.s^{-2}$
T	Temperature (K)
C	mass fraction ($J.Kg^{-1}.K^{-1}$)
t	time (s)
k	thermal conductivity ($W.m^{-1}.K^{-1}$)
(r,z)	Dimensionless coordinates
Gra_C	Massive grashof
Gra_T	Thermal Grashof
Re	Reynolds number
Pe_T	number of thermal peclet
Pe_C	number of mass peclet
H	dimensionless length
Vr	speed at the entrance
Ve_z	exit speed
$S(\theta,C)$	Non-proprietary source
C_P,	constant pressure thermal capacity
Greek Symbols	
ρ_L	reference density of fluid, $Kg.m^{-3}$
β_T	Coefficient of thermal expansion, K^{-1}
β_C	Coefficient of mass expansion,
∇	Operator Nabla
ψ	current function
ω	vorticity
$\Sigma(\theta,C)$	Adimensional source